*J. Comput. Appl. Res. Mech. Eng. Vol. 13. No. 1, pp. 55-66, 2023* *DOI:10.22061/JCARME.2023.8697.2169*

Journal of Computational and Applied Research in Mechanical Engineering
jcarme.sru.ac.ir
SRTTU
JCARME
ISSN: 2228-7922

**Research paper**

# Effect of valve plate silencing grooves on flow and pressure fluctuation in fixed displacement radial piston pump

**Lokesh Kumar*** **and Nimai Pada Mandal**

*Department of Mechanical Engineering, National Institute of Technology Patna, Patna, Bihar, 800005, India*

**Article info:**

**Article history:**

Received: 18/12/2021
Accepted: 15/02/2023
Revised: 17/02/2023
Online: 19/02/2023

**Keywords:**

Radial piston pump,
Silencing grooves,
Valve plate,
Number of pistons,
Flow and pressure fluctuation.

***Corresponding author:**
*lokesh.me15@nitp.ac.in*

**Abstract**

This study focuses on the flow and pressure fluctuations of a fixed displacement radial piston pump with a valve plate with silencing grooves, and the effect of the number of pistons (5, 6, and 7) is investigated. Over the manifolds of the pump, valve plate silencing grooves are regarded as Top Dead Center and Bottom Dead Center. The mathematical modeling is run in MATLAB Simulink. Analyzing the flow characteristics and volumetric efficiency of the pump with and without silencing groove valve plate configuration of the pump is done. The opening and closing area pattern of the kidney port is also analyzed. The percentage reduction of flow and pressure fluctuation with the silencing groove is 19% and 16.16%, respectively, for Z = 7, as compared to the model without silencing groove valve plate. The volumetric efficiency of the model with silencing groove valve plate is improved from 1% to 2% as compared to the model without silencing groove valve plate. The lower the flow and pressure fluctuation coefficients, the higher the flow rate and volumetric efficiency of the pump for the model with silencing groove valve plate.

## 1. Introduction

The radial piston pump is widely used to deliver the pressurized oil in the hydraulic system. It has many advantages over other pumps, such as higher displacement, higher operating pressure, and long life [1]. Thus, the role of the radial piston pump is significant in industrial applications; for example, widely used in machine tools, plastic and powder injection modeling system, and high-speed car drive systems [2]. This pump operates at high pressure with less noise [2], and its performance is highly dependent on non-dimensional parameters, such as flow ripple and pressure fluctuations. Cai and Tian [3] worked on the shaft assignment of the radial piston pump and observed reduced noise, higher pressure, and improved service life. Li *et al.* [4] used a CFD and a mathematical model to analyze the piston chamber's oil pressure in the radial piston pump pre-compression area. They advised against making the bottom edge's length and span angle of the triangular groove too long

or short. Guo *et al.* [5] studied the flow characteristics of a radial piston pump using the spool valve distribution technique and got a reduced flow ripple. Zhao *et al.* [6] looked into the pentagon transmission mechanism of the pump piston, built a new double-row radial piston pump, and studied flow fluctuation with greater volumetric efficiency. Tong *et al.* [7] studied the mechanism of the sliding valve distribution in the radial piston pump and analyzed the pump's piston displacement and flow characteristics. The energy-efficient design of the radial piston pump saves costs, improves durability, reduces maintenance, lowers noise, and increases stability in challenging conditions [8].

Mandal *et al.* [9, 10] investigated the influence of silencing groove geometry on the valve plate on the piston kidney of the axial piston pump. Cho *et al.* [11] looked into dynamic modeling and developed valve plate indexing with appropriate parameters to manage the pressure in the piston's transition zone and study the pump's dynamic characteristics. Seeniraj *et al.* [12] investigated numerous valve plate design strategies for noise reduction. The estimated noise reduction without influencing volumetric efficiency by combing pre-compression grooves, pre-compression filter volume with groove, and decompression filter volume on the valve plate. To optimize the piston chamber capacity of the radial piston pump the noise and pressure pulsation should be eliminated. Jiang *et al.* [13] conducted mathematical modeling in the pre-compression and decompression sectors. Huang *et al.* [14] studied pump-supplied pressure pulsation and pump characteristics using variable displacement and speed pumps. Radial piston pumps are frequently employed as output motors for hydrostatic transmissions due to their higher efficiency and low starting torque [15].

Furthermore, some experts have done studies on the hydraulic piston pump. Chao *et al.* [16] explained the mechanism of capped pistons and designed it to improve the flow characteristics of axial piston pumps, enhance the volumetric efficiency, and reduce the flow and pressure ripple. Yin *et al.* [17] studied the pressure, flow, and vibration characteristics of a seawater axial piston pump. They estimated the pressure ripple and vibration of the pump under varied loading circumstances. Nizhegorodov *et al.* [18] built a radial-piston pump and used seismic testing to identify natural frequencies for flow control. Dong *et al.* [19] designed and manufactured the valve plate of the radial piston pump and improved the efficiency of the hydraulic transmission system. They also studied the control system on the variable-displacement radial piston pump and validated a good test result. Harrison and Edge [20] proposed that the reduction of airborne noise and pressure ripple has an effect on flow ripple. The flow ripple decreases as the pump frequency increases. Ye *et al.* [21] optimally designed the valve plate to effectively reduce noise from both fluid-borne noise and structure-borne noise sources. Additionally, they proposed that the ripples in the inlet and outlet flow, as well as the pulsation of the swash plate moment, have an impact on the noise of an axial piston pump. Zhou *et al.* [22] designed the valve plate for the even number of pistons in an axial piston pump and compared it to the odd number of pistons. They discovered a minor difference in pressure pulsation between the nine- and ten-piston model pumps, as well as a decrease in pressure pulsation with increasing operating pressure in general. Tao *et al.* [23] studied mathematical modeling and simulation to mechanically design a variable displacement radial piston pump to power a large-scale, multi-megawatt wind turbine. Zielinski *et al.* [24] developed a low-speed radial piston pump to examine the hydrostatic transmission system of a small hydropower facility. The flow parameters, performance, and efficiency of the pump have been determined using simulations and mathematical analysis. They indicated that the mechanism might operate more effectively at low speeds. Aligoodarz *et al.* [25] performed mathematical modeling and simulation of the centrifugal slurry pump to find the flow characteristics and efficiency of the slurry pump. The size, concentration, and density of the solid particles have an impact on the head and efficiency of this slurry pump.

In this study, the effect of valve plate model with silencing grooves on the flow and pressure fluctuations, as well as changing pistons number

(5, 6, and 7) in the radial piston pump are analyzed. Moreover, mathematical modeling is developed and simulated with MATLAB Simulink.

## 2. Working principle of radial piston pump

A fixed displacement radial piston pump with structural details is shown in Fig. 1. The main components of the pump are cylindrical block (A), cylinder barrel (B), pump piston (C), compressed spring (D), stroking ring (E), delivery chamber (F), delivery port (G), kidney port (H), suction chamber (I), suction port (J), shaft (K) and silencing groove (M).

The cylinder block (A) is coupled with the driving shaft (K) and rotates in a journal bearing, while the pump piston (C) reciprocates with the compressed spring (D) in the cylinder barrel (B), which is positioned radially in the revolving cylinder block (A). The cylindrical geometry of valve plate and manifolds have higher and lower pressure chamber, which is referred to as delivery chamber (F) and suction chamber (I), and corresponding ports are delivery port (G) and suctions port (J). Reservoir and ports are connected through hosepipe externally. The stroking ring (E) is eccentrically fixed with the pump's outer casing and the cylindrical block. The center of eccentrically fixed stroking ring and cylinder block are 'Cs' and 'Cp,' respectively. The manifold chamber is internally connected with the kidney port (H) of the piston-cylinder barrel.

For the pump simulation, modeling considers an even and an odd number of pistons, and the number of pistons is 5, 6, and 7 for different combinations with valve plates. Pistons are labelled as 1 to 7, shown in Fig. 1, and pistons are reciprocating towards the center (Cp) of the rotating cylinder block (A) and inside the cylinder barrel (B) with deriving shaft (K). Pistons move in the direction of Top Dead Center (TDC) to Bottom Dead Center (BDC). The cylinder barrel volume reduces, and delivery stroke is accomplished. Similarly, piston movement from BDC to TDC referred toward increment in volume and accomplished the suction stroke. At full load, the area of the needle valve is $16.67 \times 10^{-6}$ m$^2$.

## 3. Mathematical modeling

In Fig. 1, Structural details of the fixed displacement radial piston pump are shown. The center of the rotating cylinder block and the cylinder barrel are considered Cp. The stroking ring (E) is fixed with the pump's outer casing, and the center of the stroking ring is Cs. The distance between the center of the cylinder block and the stroking ring is eccentricity along the y-direction, represented by the symbol $e_s$. The pistons reciprocate in the cylinder barrel, from zero to maximum from TDC to BDC, and the maximum reciprocating distance is twice the eccentricity. When the cylinder block rotates from point TDC to point, 'Os,' the angular position is covered for ith piston, with the constant rotating speed of the driving shaft. The pistons reciprocate inside the cylinder barrel with a compressed spring and rotate closely with toughing stroke ring.

The $i^{th}$ instantaneous pistons displacement of radial piston pump expressed by the Eq. (1) respectively as:

$$S_{pi} = l_m - r_i \tag{1}$$

where the $l_m$ is the length from center of cylinder block $C_p$ and the TDC of the stroking ring $r_i$ is the instantaneous linear position of the piston at contact point $O_s$.

In Fig. 1, the tringle $C_pC_sO_s$, the instantaneous linear position of the piston, can be written as;

$$r_i = e_s \cos\theta_i + r_s \cos\varphi_i \tag{2}$$

where $\varphi_i = \sin^{-1}(\frac{e_s}{r_s}\sin\theta_i)$, and $\theta_i = \theta + 2\pi(i-1)/Z$

in which Z is the number of pistons.

The $i^{th}$ instantaneous pistons velocity of the pump expressed by Eq. (3) [2] as:

$$v_{pi} = e_s\omega(\sin\theta_i + \frac{e_s}{2r_s}\sin 2\theta_i) \tag{3}$$

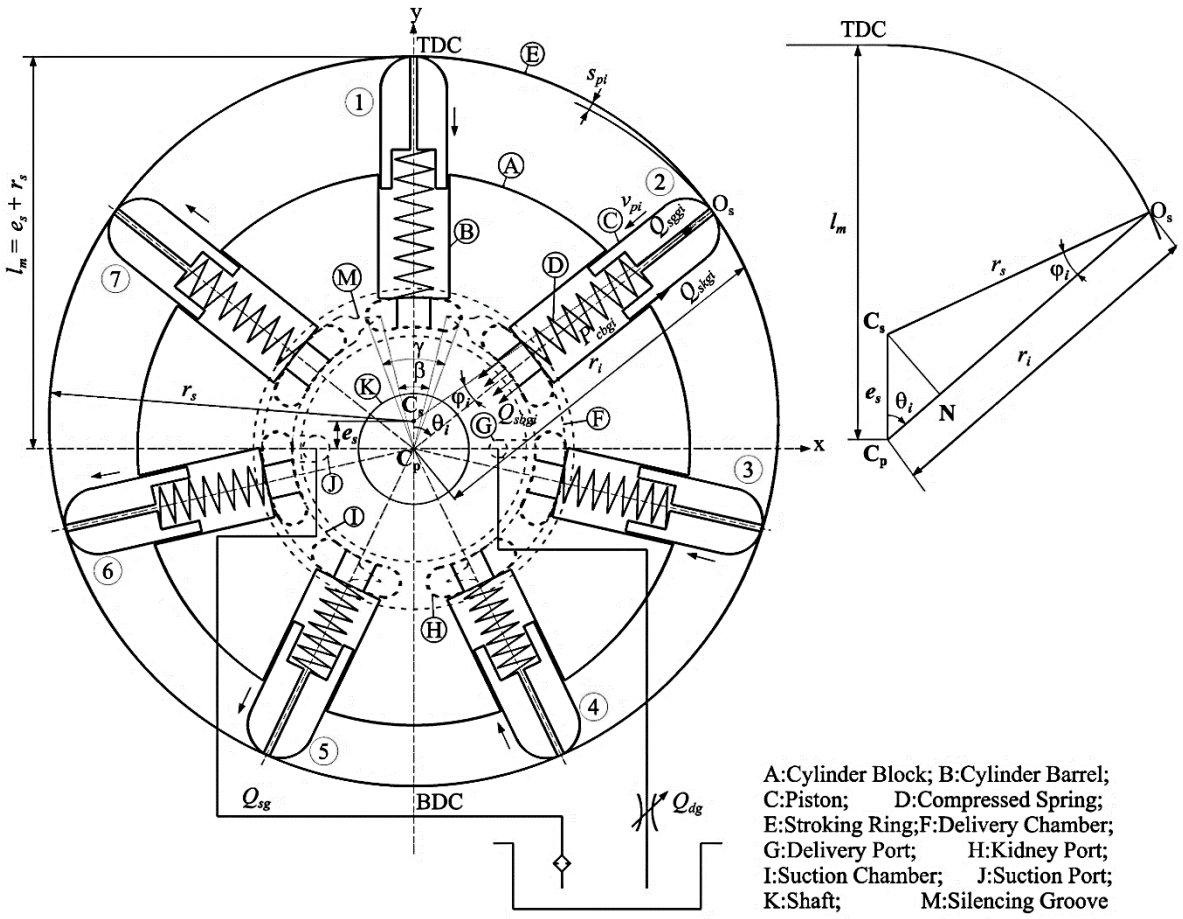


**Fig. 1.** Schematic diagram of radial piston pump with kinematic [2].

In Eq. (3), $e_s$ is the eccentricity between of stroke ring and the cylinder block in m, $r_s$ is the radius of the stroke ring in m, $\omega$ is the shaft speed in rad/s, the total number of pump pistons are Z = 5, 6, and 7, and the offset angle in between the piston is $\varphi = 2\pi/Z$.

Initially, all cylinder barrels are filled with liquid, and the initial pressure is 0.2 MPa (same as reservoir pressure). The instantaneous pressure of the $i^{th}$ cylinder barrel is the function of main flows, leakages, respective position, and instantaneous volume of the piston. The rate of instantaneous pressure of $i^{th}$ cylinder barrel for with silencing groove valve plate model can be written as in Eq. (4).

$$\frac{dP_{cbgi}}{dt} = \kappa(Q_{sgi} + A_p v_{pi} - Q_{dgi} - Q_{skgi} - Q_{sggi} - Q_{sbgi}) / (V_{pi} - A_p S_{pi}) \quad (4)$$

where $P_{cbgi}$ is the instantaneous cylinder barrel pressure, $\kappa$ is the bulk modulus, $A_p$ is the piston area, $v_{pi}$ is the instantaneous velocity of piston, $Q_{sgi}$ is the suction flow, $Q_{dgi}$ is the delivery flow, $Q_{skgi}$, $Q_{sggi,}$ *and* $Q_{sbgi}$ are the leakage flow, and $S_{pi}$ is the instantaneous displacement for $i^{th}$ piston. Similarly, the instantaneous pressure rate of $i^{th}$ piston for without silencing groove Eq. (5) is written as:

$$\frac{dP_{cbwi}}{dt} = \kappa(Q_{swi} + A_p v_{pi} - Q_{dwi} - Q_{skwi} - Q_{sgwi} - Q_{sbwi}) / (V_{pi} - A_p S_{pi}) \quad (5)$$

where $Q_{swi}$ is the suction flows and $Q_{dwi}$ is the delivery flow.

According to the elementary orifice flow equation,. described by Manring [15], the suction flows are $Q_{sgi}$ and $Q_{swi}$ for with silencing groove and with silencing groove valve plate, respectively, which are as follows:

$$Q_{sgi} = C_d A_{sgi} \sqrt{2(|P_{spg} - P_{cbgi}|) / \rho}\ sign(P_{spg} - P_{cbgi}) \quad (6)$$

$$Q_{swi} = C_d A_{swi} \sqrt{2(|P_{spw} - P_{cbwi}|)/\rho}\ sign(P_{spw} - P_{cbwi}) \quad (7)$$

Similarly, delivery flows are represented by $Q_{dgi}$ and $Q_{dwi,}$ for with silencing groove and without silencing groove valve plate model, respectively, which are as follows:

$$Q_{dgi} = C_d A_{dgi} \sqrt{2(|P_{cbgi} - P_{sg}|)/\rho}\ sign(P_{cbgi} - P_{sg}) \quad (8)$$

$$Q_{dwi} = C_d A_{dwi} \sqrt{2(|P_{cbwi} - P_{sw}|)/\rho}\ sign(P_{cbwi} - P_{sw}) \quad (9)$$

where $P_{spg}$ and $P_{spw}$ are the suction manifold pressures, $P_{sg}$ and $P_{sw}$ are the delivery manifold pressures, $A_{sgi}$ and $A_{swi}$ are the instantaneous piston kidney area at suction side, $A_{dgi}$ and $A_{dwi}$ are the instantaneous piston kidney area at delivery side for with silencing groove and without silencing groove valve plate model, respectively.

The instantaneous pressure rate of delivery manifold of the pump for with silencing groove configuration can be written as:

$$\frac{dP_{sg}}{dt} = (\sum_{i=1}^{5} Q_{dgi} - Q_{dg})\kappa / V_d \quad (10)$$

where $Q_{dg}$ is the discharge through the needle and $V_d$ is the pipe line volume up to needle valve. Similarly, the supply pressure rate of the delivery manifold chamber of the pump without silencing groove valve plate model is replaced with symbols $P_{sw}$, $Q_{dwi}$, and $Q_{dw}$, using Eq. (10).

The flow through the needle valve orifice with silencing groove valve plate model can be written as in Eq. (11) [15].

$$Q_{dg} = C_d A_{ng} \sqrt{2(P_{sg} - P_r)/\rho}\ sign(P_{sg} - P_r) \quad (11)$$

Similarly, flow through the needle valve orifice $Q_{dw}$ without silencing groove valve plate model is replaced with symbols $P_{sw}$ and $A_{nw}$ using Eq. (11); where $A_{ng}$ and $A_{nw}$ are the areas of needle valve and $P_r$ is reservoir pressure.

The Eqs. (4 and 5) shown for the valve plate with silencing groove and without silencing groove models are dependent on leakage flows of the pump, in between the annular gap of piston and barrel cylinder, central orifice of the piston and cylindrical valve plate and cylinder block. It can help the lubricating of systems and improve the anti-wear property. Equations from Eqs. (1-4) and Eqs. (12-16) are taken from Ivantysyn and Ivantysynova [2].

The leakage between the annular gap of the $i^{th}$ piston and barrel cylinder (Eq. (12)), through the central orifice of the $i^{th}$ piston (Eq. (13)), and between the annular gap of the cylindrical valve plate and $i^{th}$ cylinder block (Eq. (14)) are proposed by Ivantysyn and Ivantysynova [2].

$$Q_{skgi} = \frac{\pi d_k h_k^3}{12\mu l_k}(P_{cbi} - P_r) - \mu d_k h_k v_{pi} / 2 \quad (12)$$

$$Q_{sggi} = \frac{\pi d_d^4}{128\mu l_d}(P_{cbgi} - P_r) \quad (13)$$

$$Q_{sbgi} = \frac{h_g^3}{12\mu}(P_i - P_r)\int d\delta / L \quad (14)$$

where $d_k$ is the diameter of cylinder, $h_k$ is the clearance between piston and barrel cylinder, $P_{cbgi}$ is the $i^{th}$ cylinder barrel pressure, $l_k$ is the path length of piston in cylinder, $\mu$ is the oil dynamic viscosity, $l_d$ is the length of central orifice of piston, $d_d$ is the diameter of circular hole in piston, $h_g$ is the clearance between valve plate and cylinder block, $L$ is the width of manifold path is taken constant, and the $d\delta$ is the function of angular position of width of manifold path.

## 4. Results and discussion

The instantaneous piston kidney area over the manifold is connected to the delivery side and the suction side area, as shown in Fig. 2.

The delivery side of the piston kidney areas are indicated with $A_{dgi}$ and $A_{dwi}$ for with and without silencing groove, respectively, and their corresponding expression are given in Eqs. (8 and 9). Similarly, with and without silencing groove, piston kidney areas in the suction side are represented with $A_{sgi}$ and $A_{swi}$, given in Eqs. (6 and 7), respectively.

The piston kidney area is calculated with the parametric value of piston and kidney and is mentioned in Table 1.

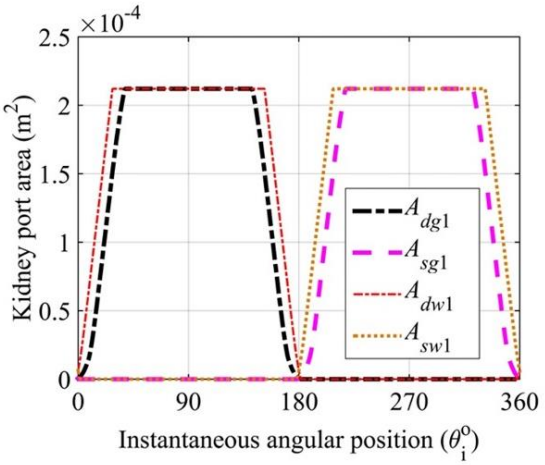


**Fig. 2.** Instantaneous kidney port area variation of 1st piston over the manifold.

**Table 1.** Parametric values used in simulation.

| Parameter | Value |
|---|---|
| Volumetric displacement (for Z=5, 6, and 7 pistons) [8] | 63, 76, and 89 cc/rev |
| Pitch radius of manifold (m) | 0.05 m |
| Kidney port radius (m) | 0.0043 m |
| Silencing groove angle (rad) | $\pi/9$ |
| Kidney port angle (rad) | $\pi/6$ |
| Angle of bridge gap (rad) | $13\pi/90$ |
| Eccentricity in cylinder block (m) | 0.012 |
| Diameter of piston (m) | 0.026 |
| Initial volume of cylinder ($m^3$) | $1.5 \times 10^{-5}$ |
| Control volume of delivery manifold ($m^3$) | $3 \times 10^{-4}$ |
| Control volume of suction manifold ($m^3$) | 0.76 |
| Dead volume of cylinder ($m^3$) | $2.5 \times 10^{-6}$ |
| Reservoir pressure (MPa) | 0.2 |
| Coefficient of discharge of port | 0.61 |
| Bulk modulus of fluid ($N/m^2$) [10] | $8.547 \times 10^8$ |
| Density of fluid (kg /$m^3$) [10] | 860 |
| Needle valve dimeter on delivery side (m) | $4.6 \times 10^{-3}$ |

Simulation is run in MATLAB, and S- function is used for calculating the piston kidney area. For this calculation Runge-Kutta solver and $1e^{-7}$ s fixed time step are used. Half of the cycle works for the delivery port, and another half for the suction port. This kind of cyclic opening and closing of the kidney port area continuously happens for every piston. In Fig. 2, up to 180-degree delivery port is opened, while this duration suction port is closed after 180 degrees, the suction port is opened, and the delivery port gets closed.

At 180 degrees, the main difference is that the silencing groove port area is open smoothly compared to without silencing groove, which has a sharp opening. Sharp opening promotes the fluctuations. Initially, the piston is fitted with the compressed spring and reciprocating in the cylinder barrel and stroke ring. The cylinder block rotated with the pump shaft and piston reciprocating at a constant rotational speed in the cylinder barrel. The cylinder kidney and cylinder of the pump moved over the manifolds from the TDC, i.e., $\theta = 0^0$, to the BDC, i.e., $\theta = 180^0$, which is known as the delivery manifold.

The cylinder volume diminishes since the piston reciprocates within the cylinder barrel, and fluid flows from the cylinder barrel to the delivery manifold. Taking after the completion of the half cycle, known as suction, from BDC, i.e., $\theta = 180^0$, to TDC, i.e., $\theta = 360^0$ or $0^0$, since the volume of the barrel expanded with the precise position in this area. Pump piston displacement affects the volumetric displacement of the pump. The instantaneous displacement and velocity (at 1500 rpm) curve of the pump for a single cycle is shown in Fig. 3, and the displacement and velocity of the pump are calculated with the help of Eq. (1 and 3), respectively.

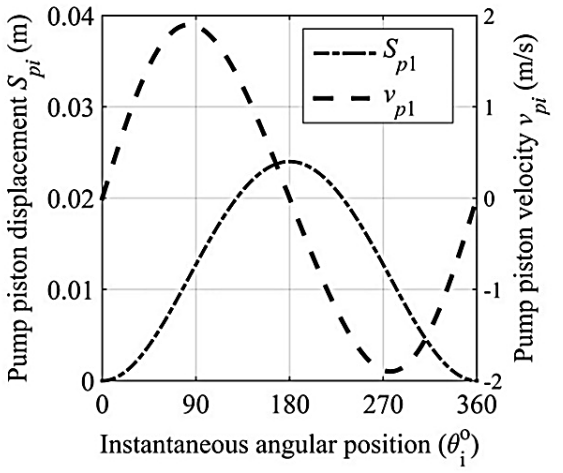


**Fig. 3.** Pump piston displacement and velocity curve at the speed of 1500 rpm.

The maximum displacement of the piston is twice the eccentricity between the cylinder block and stroke ring. The maximum pump piston velocity is 1.898 m/s. The pump cylinder barrel pressure is dependent on the kinematic of the piston and fluid flow from manifolds to the cylinder barrel and vice versa, as shown in Eq. (5). For the without-silencing groove valve plate model of the pump shown in Fig. 4, the supply pressure ($P_{sw}$), cylinder barrel pressure ($P_{cbw1}$), and suction pressure ($P_{spw}$) are built-up in the delivery manifold, cylinder barrel, and suction-manifold, respectively, and the needle valve orifice area is $16.67 \times 10^{-6}$ m$^2$. These pressures are estimated at 1500 rpm with 7 pistons (Z = 7) and 1.5 cycles for the valve plate without silencing groove. The maximum supply and cylinder barrel pressures are 10.2 MPa and 10.23 MPa, respectively. Eq. (11), for both the model with and without the silencing groove valve plate model at the same load area of the needle valve, defines the pump flow rate via the needle valve. Fig. 5 shows the instantaneous flow rate through a needle valve without a silencing groove at 1500 rpm, with a varying number of pistons models (i.e., Z= 5, 6, and 7) and a pressure of 10 MPa. With a silencing groove model, the mean flow rates are 93.23 lpm, 112.1 lpm, and 130.7 lpm, while without a silencing groove; the mean flow rates are 92.6 lpm, 110.9 lpm, and 129.3 lpm, with 5, 6, and 7-piston model of the pump, respectively. These simulated radial piston pump results are validated at pressures ranging from 5 to 25 MPa, with a mean flow rate of the same volumetric displacement as the Moog pump catalog [8], as illustrated in Fig. 6 at 1500 rpm. The simulated model's mean flow ranges from 88.39 lpm to 93.67 lpm for without silencing groove model at pressures ranging from 5 MPa to 25 MPa for 5 pistons, while the Moog pump's mean flow ranges from 93,85 lpm to 89 lpm [8]. For the 6-piston model without silence groove and silencing groove, the mean flow ranges from 112.6 lpm to 106.4 lpm and from 113.5 lpm to 108 lpm, respectively. The mean flow rate is changed from 131.3 lpm to 124 lpm for the model without silencing groove and from 132.2 lpm to 125.9 lpm for the model with silencing groove, respectively, at the same pressure range depicted in Fig. 6.

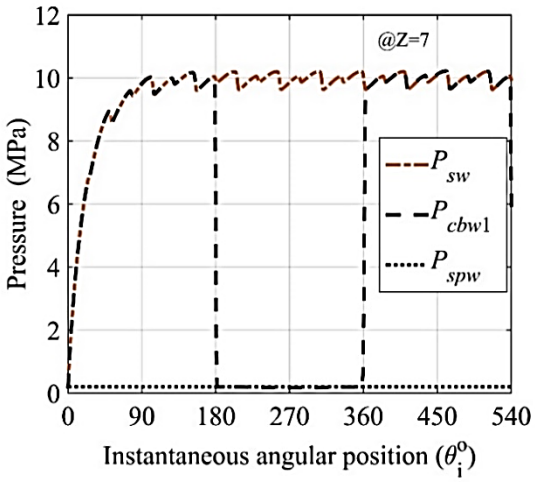


**Fig. 4.** Pressure characteristics of the pump for without silencing groove model at the speed of 1500 rpm.

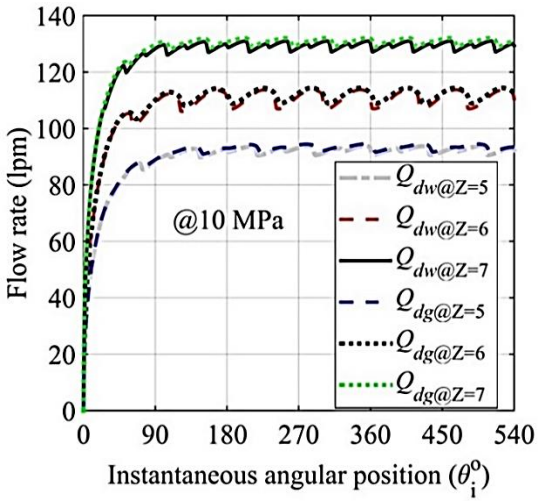


**Fig. 5**. Flow characteristics of the pump at the speed of 1500 rpm for silencing groove model.

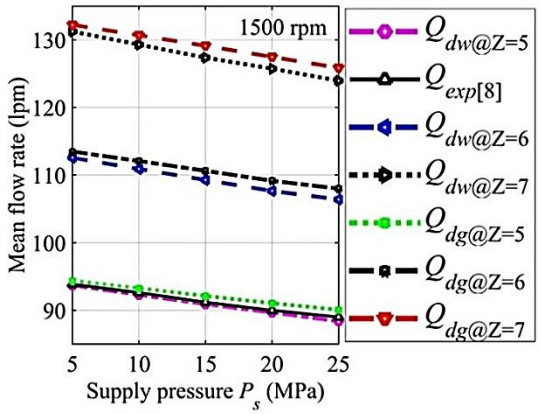


**Fig. 6.** Mean flow rate of the pump with supply pressure at the speed of 1500 rpm.

The positive displacement piston pump creates internal vibration due to cyclic loads caused by the fluid pressure in the cylinder barrel, which is liquid at high pressure.

The pump manifolds transmit these vibrations to the remainder of the hydraulic system, creating vibration in the component and airborne noise from the pump valve plate geometry. The flow fluctuation of fluid through the valve plate geometry creates two types of noise known as "airborne noise" and "structure-borne noise". The flow ripple in terms of non-dimensional parameter analysis at different speeds and the same load area of a needle valve for 5, 6, and 7 piston modeled at a rate of 1500 rpm, 1800 rpm, and 2100 rpm for without and with silencing groove, respectively, is shown in Fig. 7. For the silencing groove model, Ivantysyn and Ivantysynova [2] and Zhao *et al.* [6] define this ripple in the percentage of flow fluctuation coefficient, which is written as Eq. (15).

$$\delta_{qg} = \{\{(Q_{dg})_{\max} - (Q_{dg})_{\min}\} / (Q_{dg})_{mean}\} \times 100\% \quad (15)$$

where $(Q_{dg})_{\max}$ is the maximum steady-state flow rate, $(Q_{dg})_{\min}$ is the minimum steady-state flow rate, and $(Q_{dg})_{mean}$ is the mean steady-state flow rate. Similarly, the flow fluctuation coefficient ($\delta_{qw}$) for without silencing groove is used by Eq. (15) and the flow coefficient at different speeds is calculated using different piston number models, as shown in Fig. 7. The theoretical flow rate fluctuation coefficient in terms of non-uniformity grade can be written in Eq. (16).

$$\delta_{tq} = \varphi_Z \tan(\varphi_Z / 2) \quad (16)$$

where $\varphi_Z = 180^o / Z$ in case of an even number of pistons, $\varphi_Z = 90^o / Z$ in case of an odd number of pistons, and $\varphi_Z$ is the angle between the minimum and maximum theoretical flow rate. The theoretical flow fluctuation coefficient values for 5, 6, and 7 piston models are 0.049, 0.14, and 0.025, respectively, calculated by Ivantysyn and Ivantysynova [2]. As the number of pistons (odd or even) at the same speed increases, the theoretically and calculated simulated fluctuation coefficient decreases. The flow fluctuation coefficient for using an even number of pistons is mathematically larger than for using an odd number of pistons, as shown in Fig.7. The increased rotation speed of the pump reduces flow fluctuation. The flow fluctuation coefficient decreases for Z = 5, and for the model of valve plate with a silencing groove compared to the without a silencing groove are 12.67%, 9.77%, and 8.4% at the speeds of 1500 rpm, 1800 rpm, and 2100 rpm, respectively. Similarly, the flow fluctuation coefficient decreases for the silencing groove valve plate model as compared to the without silencing groove, which are 22%, 18.64%, and 16.76% for Z = 6, and 19%, 15.70%, and 13.94% for Z = 7, at the same speed. The flow fluctuation coefficient at the speed of 1500 rpm with a different load pressure ranges from 5 MPa to 25 MPa, considering the pump's 5, 6, and 7 piston model without silencing groove and with silencing groove model, respectively, are shown in Fig. 8.

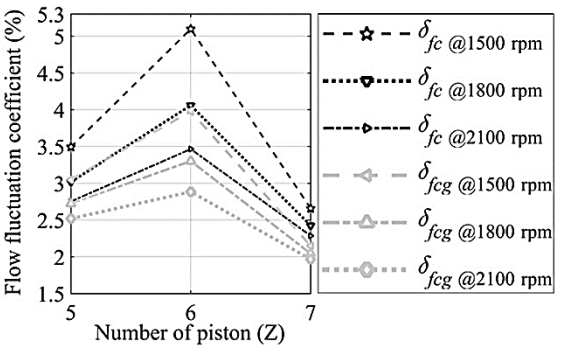


**Fig. 7.** Flow fluctuation coefficient with velocity variation.

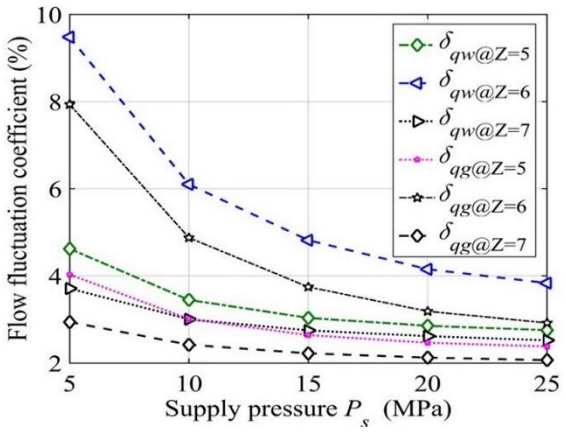


**Fig. 8.** Flow fluctuation coefficient of the pump at different loads at the speed of 1500 rpm.

The overall range of flow fluctuation is 9.5% to 2.06% for Z = 5, 6, and 7 at the pump's wide supply pressure range at 1500 rpm. The range of flow fluctuation within the silencing groove is from 4.03% to 2.33% for Z = 5, from 7.94% to 2.92% for Z = 6, and from 2.94% to 2.06% for Z = 7 at the same pressure range and speed. Similarly, for the model without a silencing groove, the range of flow fluctuation is 4.62%–2.75%, 9.5%–3.84%, and 3.71%–2.52% for Z = 5, 6, and 7, respectively.

The fluid flow inside the pump component, such as fluid flow from the cylinder barrel to the manifolds and vice versa, is combined with ripples to create wave propagation. This propagation raises pressure of the system on a regular basis, reducing pump life. The supply pressure fluctuation coefficient is a non-dimensional measure that expresses the pressure ripple. This analysis is performed at different speeds such as 1500 rpm, 1800 rpm, and 2100 rpm, for with and without silencing groove with the consideration of 5, 6, and 7 number of the piston at a fixed area of the needle valve, shown in Fig 9. Huang *et al.* [14] characterized the pressure ripple as a non-dimensional parameter represented by Eq. (17).

$$\psi_{pg} = \{\{(P_{sg})_{\max} - (P_{sg})_{\min}\} / (P_{sg})_{mean}\} \times 100\% \quad (17)$$

where, $(P_{sg})_{\max}$ is the steady-state maximum supply pressure of pump, $(P_{sg})_{\min}$ is the steady-state minimum supply pressure of pump, and $(P_{sg})_{mean}$ is steady-state mean supply pressure of pump.

Similarly, the pressure fluctuation coefficient ($\psi_{pw}$) for without silencing groove model is used by Eq. (17) and the pressure fluctuation coefficient is calculated at different speeds using different piston number models shown in Fig 9. The pressure fluctuation also decreases as the odd or even number of pistons increases. This fluctuation reduces with increased pump speed. The reduction of the pressure fluctuation coefficient of the with-silencing groove valve plate model compared to the without-silencing groove model is 12.65%, 9.78%, and 8.49% using Z = 5, 6, and 7, respectively, at 1500 rpm. Similarly, the pressure fluctuation reduction in the model with silence groove versus the model without silence groove is 21.91%, 18.64%, and 16.8% for z = 6 and 16.16%, 15.73%, and 13.93% for z = 7, as shown in Fig 9.

The pressure fluctuation coefficient analysis at the speed of 1500 rpm, for further pressure, ranges from 5 MPa to 25 MPa, considering the pump's 5, 6, and 7 piston model without silencing groove and silencing groove model, respectively, as shown in Fig. 10. This shows the pressure fluctuation coefficient decreases with an increased range of supply pressure from the pump and a different number of pump pistons. The range of pressure fluctuation for the model with a silencing groove is 7.7% -4.72%, 15.08 - 5.78%, and 5.623% -4.096% at the range of 5 MPa to 25 MPa pressure of the pump. Similarly, at the same wide range of pump pressure, the pressure fluctuation range for the pump model without a silencing groove is 8.83%-5.46%, 18%-7.58%, and 7.08%-5% for Z = 5, 6, and 7 pistons, respectively.

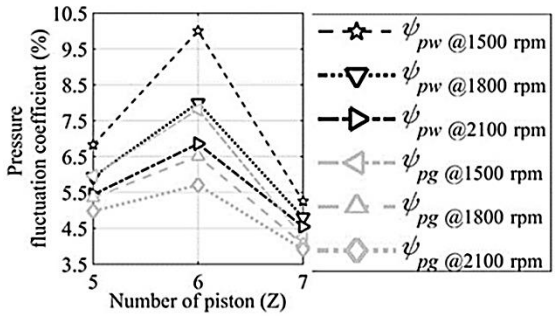


**Fig. 9.** Pressure fluctuation coefficient variation with number of pistons.

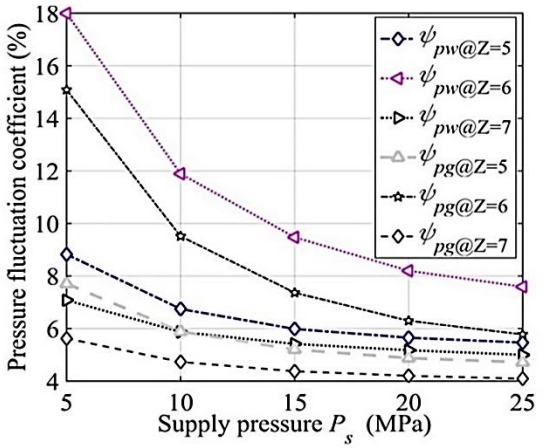


**Fig. 10**. Pressure fluctuation coefficient of the pump at different loads at the speed of 1500 rpm.

The pump capacity is expressed in the term of volumetric efficiency, and its equation is expressed in Eq. (18) for silencing groove model.

$$\eta_{vg} = (Q_{dg} / Q_t) \times 100\% \quad (18)$$

Similarly, the volumetric efficiency is represented as ($\eta_{vw}$), and discharge with $Q_{dw.}$ for without silencing groove model.
Theoretical flow rate of pump is expressed by Eq. (19) [2].

$$Q_t = 0.5 Z \omega e_s \pi d_k^2 \quad (19)$$

where $Q_{dg}$ and $Q_{dw}$ are the mean flow rate of needle valve, with and without silencing groove model, respectively. Z is the number of pistons, ω is the pump speed, $e_s$ is the eccentricity between cylinder block and stroking ring, and $d_k$ is the diameter of piston of pump.
Fig. 11 depicts the percentage of volumetric efficiency with different supply pressure at the speed of 1500 rpm considering 5, 6, and 7 pistons of the model for both with silencing groove and without silencing groove model, respectively. The volumetric efficiency decreases with an increased supply pressure of the pump. The volumetric efficiency between 98.95% to 92.49% at supply pressure ranges from 5 MPa to 25 MPa.

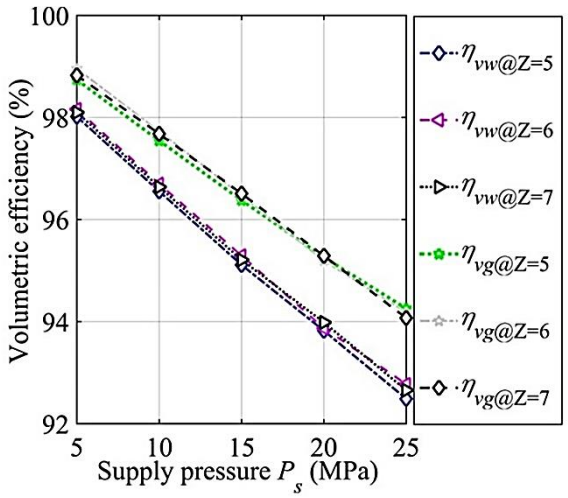


**Fig. 11**. Volumetric efficiency of the pump at different loads at the speed of 1500 rpm.

Using a silencing groove, the volumetric efficiency is improved over a valve plate model without a silencing groove for a wide range of supply pressure. The volumetric efficiency for the pump model with a silencing groove valve plate, using Z = 5, 6, and 7 pistons, is 98.74%-94.26%, 98.95%-94.18%, and 98.82%-94.07%, respectively. Similarly, for the same supply pressure range, the volumetric efficiency of the pump without a silencing groove valve plate, using Z = 5, 6, and 7 pistons, is 98.02%-92.49%, 98.16%-92.78%, and 98.1%-92.66%, respectively, as shown in Fig. 11.

## 4. Conclusions

This study looks into the impact of valve plate silencing grooves on flow and pressure fluctuation in fixed displacement radial piston pumps with 5, 6, and 7 pistons. The following conclusions are made:

- When silencing grooves are used, the opening and closing areas of the kidney port are smoother than in models without silencing groove valve plates.
- The effect is significantly less when comparing the flow rate with and without silencing grooves for an equivalent number of pistons.
- The mean flow rate is higher in every situation, where silencing grooves are used, and a maximum flow rate of 7 pistons is obtained.
- At various speeds (1500, 1800, and 2100 rpm) and supply pressures, a minimum flow and pressure fluctuation are reported for seven pistons (up to 25 MPa). However, the highest fluctuation is found in the case of 6 piston numbers.
- When silencing grooves are used in the valve plate, volumetric efficiency is higher than in the model without silencing grooves, and maximum efficiency is found at 7 pistons in the silencing groove scenario.

## References

[1] J. Yuehu, "New type of radial piston pump", *National defence Ind. Press*, Beijing, pp. 6–8, (2012).

[2] J. Ivantysyn and M. Ivantysynova, *Hydrostatic Pumps and Motors Principles, Designs, Performance, Modelling, Analysis, Control and Testing;* 1st ed, Akad. Books Internat., New Delhi, pp.185-203, (2000).

[3] H. M. Cai and M. J. Tian, "Design of a shaft assignment radial piston pump", *Adv. Mater. Res.*, Vol. 510, pp. 9-12, (2012).

[ ] S. N. Li, L. J. Wei, X. P. Wei and J. H. Yang, "Change in oil pressure in piston chamber of a radial piston pump pre-compression area hen considering the compressibility of oil", *Int. J. Fluid Mach. Syst.*, Vol. 13, No. 1, pp. 463-475, (2020).

[5] T. Guo, S. Zhao and C. Liu, "Study on flow characteristics and flow ripple reduction schemes of spool valves distributed radial piston pump", *Proc. Inst. Mech. Eng., Part C: J. Mech. Eng. Sci.*, Vol. 231, No. 12, pp. 2291-2301, (2017).

[6] S. Zhao, T. Guo, Y. Yu, P. Dong, C. Liu and W. Chen, "Design and experimental studies of a novel double-row radial piston pump", *Proc. Inst. Mech. Eng., Part C: J. Mech. Eng. Sci*, Vol. 231, No. 10, pp. 1884-1896, (2017).

[7] G. Tong, Z. Shengdun, Y. Yanghuiwen and S. Peng, "Design and theoretical analysis of a sliding valve distribution radial piston pump", *J. Mech. Sci. Technol.*, Vol. 30, No. 1, pp. 327-335, (2016).

[8] Moog Radial Piston Pumps RKP Catalog, *Online referencing*, (2018).

[9] N. P. Mandal, R. Saha and D. Sanyal, "Theoretical simulation of ripples for different leading-side groove volumes on manifolds in fixed-displacement axial-piston pump", *Proc. Inst. Mech. Eng., Part I: J. Syst. Control Eng.*, Vol. 222, No. 6, pp. 557-570, (2008).

[10] N. P. Mandal, R. Saha and D. Sanyal, "Effects of flow inertia modelling and valve-plate geometry on swash-plate axial-piston pump performance", *Proc. Inst. Mech. Eng., Part I: J. Syst. Control Eng.*, Vol. 226, No. 4, pp. 451-465, (2011).

[11] J. Cho, X. Zhang, N. D. Manring and S. . Nair, "Dynamic modelling and parametric studies of an indexing alve plate pump", *Int. J. Fluid Power*, Vol. 3, No. 3, pp. 37-48, (2002).

[12] G. K. Seeniraj, M. Zhao and M. Ivantysynova, "Effect of combining precompression grooves, PCFV and DCFV on pump noise generation", *Int. J. Fluid Power*, Vol. 12, No. 3, pp. 53-63, (2011).

[13] W. Jiang, X. G. Qiu, G. Z. Chai and J. X. Zhou, "Research of the pressure pulsation within piston chamber in radial piston pump", *Adv. Mater. Res.*, Vol. 69-70, pp. 626-630, (2009).

[1 ] J. Huang, Z. Yan, L. Quan, Y. Lan and . Gao, "Characteristics of delivery pressure in the axial piston pump with combination of variable displacement and variable speed", *Proc. Inst. Mech. Eng., Part I: J. Syst. Control Eng.*, Vol. 229, No. 7, pp. 599-613, (2015).

[15] N. D. Manring and R. C. Fales, *Hydraulic Control Systems*; 2nd ed, Wiley, New Jersey, pp. 1597-159, (2019).

[16] Q. Chao, Z. Xu, J. Tao and C. Liu, "Capped piston: A promising design to reduce compressibility effects, pressure ripple and cavitation for high-speed and high-pressure axial piston pumps", *Alex. Eng. J.*, Vol. 62, pp. 509-521, (2023).

[17] F. Yin, S. Nie, W. Hou and S. Xiao, "Effect analysis of silencing grooves on pressure and vibration characteristics of seawater axial piston pump", *Proc. Inst. Mech. Eng., Part C: J. Mech. Eng. Sci.*, Vol. 231, No. 8, pp. 1390-1409, (2017).

[18] A. I. Nizhegorodov, A. N. Gavrilin, B. . Moyzes, A. I. Cherkasov, O. M. Zharkevich, G. S. Zhetessova and N. A. Savelyeva, "Radial-piston pump for drive of test machines", *IOP Conf. Ser.: Mater. Sci. Eng.*, Vol. 289, No. 1, pp. 012014, (2018).

[19] P. Dong, S. Zhao, Y. Wang, P. Zhang, X. Han, C. Liu, D. Meng and Y. Dong, "Design and Experimental Study of Radial Piston Pump with Valve Plate Distribution", *Proc. ASME 2019, Int. Mech. Eng. Congress and Expo., Des., Syst., and Complx.*, Salt Lake City, Utah, USA, Vol. 14, No. 11-14, V014T14A035, (2019).

[20] K. A. Harrison and K. A. Edge, "Reduction of axial piston pump pressure ripple", *Proc. Inst. Mech. Eng., Part I: J. Syst. Control Eng.*, Vol. 214, No. 1, pp. 53-64, (2000).

[21] S. G. Ye, J. H. Zhang and B. Xu, "Noise reduction of an axial piston pump by valve plate optimization", *Chin. J. Mech. Eng.*, Vol . 31, No. 1, pp. 1-16, (2018).

[22] J. Zhou, C. Jing, Q. Bao and W. Wu, "Novel study on the pressure pulsation of the axial piston machines with even number of pistons", *The J. Eng.*, Vol. 2020, No. 14, pp. 932-935, (2020).

[23] M. Zielinski, A. Myszkowski, M. Pelic and R. Staniek, "Low-speed radial piston pump as an effective alternative power transmission for small hydropower plants", *Renew. Energy*, Vol. 182, pp. 1012-1027, (2022).

[24] M. R. Aligoodarz, M. Dalvandi and A. Mehrpanahi, "Solid-phase effects on the performance of a centrifugal slurry pump using computational fluid dynamics", *J. Comput. Appl. Res. Mech. Eng. (JCARME)*, Vol. 11, No. 1, pp. 243-255, (2021).

[25] M. R. Aligoodarz, M. Dalvandi and A. Mehrpanahi, "Solid-phase effects on the performance of a centrifugal slurry pump using computational fluid dynamics", *J. Comput. Appl. Res. Mech. Eng. (JCARME)*, Vol. 11, No. 1, pp. 243-255, (2021).



**How to cite this paper:**

Lokesh Kumar and Nimai Pada Mandal, "Effect of valve plate silencing grooves on flow and pressure fluctuation in fixed displacement radial piston pump,", *J. Comput. Appl. Res. Mech. Eng.*, Vol. 13, No. 1, pp. 55-66, (2023).

**DOI:** 10.22061/JCARME.2023.8697.2169

**URL:** https://jcarme.sru.ac.ir/?_action=showPDF&article=1837